Inorganic Chemistry

Article

pubs.acs.org/IC

Infinite Copper(II) Coordination Architectures from a Resonative Aminotriazine-Derived Tripodal Ligand: Synthesis, Structures, and Magnetic Properties

Meng-Jung Tsai,[†] Jing-Yun Wu,*[,†] Ming-Hsi Chiang,*[,‡] Cheng-Hao Huang,[†] Ming-Yu Kuo,[†] and Long-Li Lai*[,†]

[†]Department of Applied Chemistry, National Chi Nan University, Nantou 545, Taiwan

[‡]Institute of Chemistry, Academia Sinica, Taipei 115, Taiwan

Supporting Information

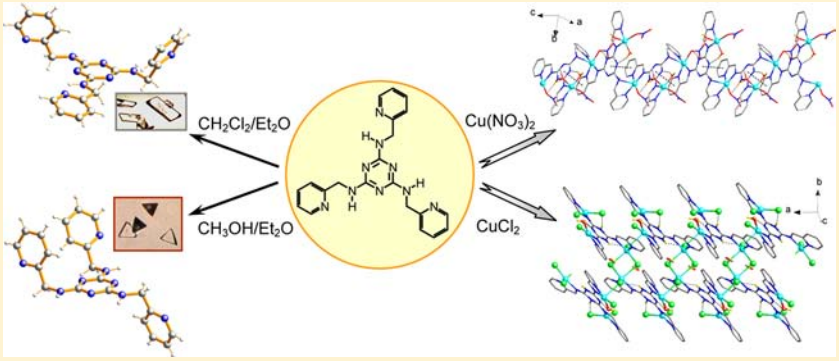

ABSTRACT: The ligand 2,4,6-tris(2-picolylamino)-1,3,5-triazine (*o*-H_3tpat) with essentially resonative structure and two copper(II)-based one-dimensional coordination chain structures, $[Cu_3Cl_5(o\text{-}H_2tpat)(H_2O)]\cdot MeOH\cdot CH_2Cl_2$ (**1**) and $[Cu_2(o\text{-}H_2tpat)(H_2O)(MeOH)(NO_3)_2](NO_3)\cdot 3MeOH$ (**2**), with different structural patterns have been synthesized and characterized using single crystal X-ray diffraction analysis. For *o*-H_3tpat, two crystalline forms showing different solid-state structural features are obtained from $MeOH/Et_2O$ (form **I**) and CH_2Cl_2/Et_2O (form **II**), respectively. The *o*-H_3tpat form **I** adopts an asymmetric-configured all-amino resonative tautomer with three *cis*−*trans*−*trans*-arranged pyridyl groups, whereas the *o*-H_3tpat form **II** adopts also an identical resonative structure but where two of the three pyridyl groups are in a *cis*-manner and the third one is nearly coplanar with the central aminotriazine core. On the other hand, the designed tripodal ligand in both Cu(II)-complexes serves as a monoanion, *o*-H_2tpat^-, which suits a propeller-configured all-imino resonative structure in **1** and a *syn*−*anti*-configured amino−imino−imino resonative structure in **2**. These observations significantly indicate that the *o*-H_3tpat ligand can self-adjust and interconvert its conformation via a possible structure transformation associated with proton-shift to adapt a change in the crystallization and self-assembly reaction systems. In the magnetic point of view, **1** is treated as repeated chains composed of infinite $\{Cu_6Cl_{10}\}$ units wherein the hexanuclear unit is further decomposed to one $\{Cu(II)_4Cl_6\}$ and two magnetically isolated $\{Cu(II)Cl_2\}$ subunits. Antiferromagnetic interactions are found for the Cu_4 subunits ($g = 2.33$, $2J_1 = -5.6$ cm^{-1}, $2J_2 = -8.6$ cm^{-1}, $2J_3 = -4.1$ cm^{-1}, and J_4 held to zero). For **2**, it is considered as an infinite chain that composes of Cu_2 units antiferromagnetically coupled ($g = 2.03$, $2J_1 = -0.2$ cm^{-1}). The small antiferromagnetic exchange constants in both **1** and **2** suggest that the unpaired spins do not effectively interact through the tripodal *o*-H_2tpat^- ligands.

INTRODUCTION

In the past decade, a tremendous effort has been devoted to the targeted construction of polymeric and/or discrete metallo-supramolecular assemblies from tailored molecular components through metal−ligand direct coordinate bonds and/or non-covalent interactions, mostly hydrogen bondings and $\pi-\pi$ stacking interactions.[1] Aminotriazine (melamine) derivatives have proven their great potential in organizing tecton-based hydrogen-bonded supramolecular networks[2−8] and in complexing with metal ions via functionalized donating groups to yield new oligo- and polynuclear metal coordination arrays with fascinating structural and spectroscopic properties, and even biological functions.[9−17] For example, the multidentate trinucleating ligand 2,4,6-tris(dipyridin-2-ylamino)-1,3,5-triazine (dpyatriz) as bidentately bound three copper(II) ions in a trigonal array via its three pairs of pyridine-N donors, giving rise to the formation of oligo-nuclear discrete cage-like structures[11,12a,17] and one-dimensional polymeric chains.[10a,12] In addition, the strong electron-withdrawing (π-deficient)

Received: July 31, 2012
Published: November 2, 2012

properties of the 1,3,5-trazine ring of aminotriazine ligands has been found to enhance the noncovalent anion−aromatic interactions between anions and the aryl centroid of π-acidic rings for the recognition of anions.[11,12,18]

Among the aminotriazine-based polydentate ligands, it is of particular interest to note that *N*-substituted secondary aminotriazine derivatives agree a large contribution of the resonative conformers up to nineteen with respect to both electronic and geometric isomerism (Scheme S1 in the Supporting Information).[19−21] In view of electronic isomerism, either amino or imino resonative structure exists as a result of heterocyclic tautomerism through the system of conjugated double bonds associated with hydrogen shift between the out-of-ring amino (N_{outer}) and inner ring nitrogen atoms (N_{inner}).[19] This dynamic process demonstrates four possibilities from an all-amino tautomer to an imino−amino−amino, an amino−imino−imino, and an all-imino tautomeric form. On the other hand, with the aspect of geometric isomerism, *N*-substituted secondary aminotriazine derivatives allow a propeller and an asymmetric conformer for the all-amino and all-imino resonative structures as well as a *syn*−*syn*, a *syn*−*anti*, and an *anti*−*anti* conformer for the imino−amino−amino and amino−imino−imino resonative structures. These conformational isomers arise from two dynamic processes: (*i*) the restricted rotation about the amino−triazine bond for the amino tautomers and (*ii*) the *E*−*Z* isomerism for the imino tautomers.[19−21] In addition, it is also worth noting that the remaining out-of-ring amine-hydrogens can serve as hydrogen donors; this may dominate complementary supramolecular recognitions in addition to their coordination features.[22−24] Therefore, the coordination chemistry of this type of aminotriazine derivatives is expected to be interesting.

Herein, we report on the synthesis, characterization, and solid-state structures of a novel tripodal *N*-substituted secondary pyridine-amine-triazine ligand, 2,4,6-tris(2-picolylamino)-1,3,5-triazine (*o*-H_3tpat, Scheme 1), following on its reactivity toward the preparation, X-ray structure characterization, and the magnetic properties of two copper(II)-based one-dimensional coordination chain arrays. The varied ligand conformations are also discussed.

Scheme 1. Molecular Structure of 2,4,6-Tris(2-picolylamino)-1,3,5-triazine (*o*-H_3tpat)

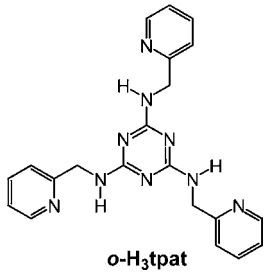

EXPERIMENTAL SECTION

Materials and Instruments. Chemical reagents were purchased commercially and were used as received without further purification. ^{1}H and ^{13}C{^{1}H} NMR spectra were recorded on a Bruker AMX-300 Solution-NMR spectrometer. All chemical shifts are reported in δ units with reference to the residual protons of the deuterated solvent. Coupling constants are given in Hertz. Matrix-assisted laser desorption ionization time-of-flight mass spectra (MALDI-TOF-MS) were measured on a Bruker Daltonics flexAnalysis mass spectrometer. Thermogravimetric (TG) analyses were performed under nitrogen with a Perkin-Elmer Pyris 1 TG analyzer. Infrared (IR) spectra were recorded on a Perkin-Elmer RX1 Fourier transform infrared spectrometer. Elemental analyses (C, H, N) were performed on an Elementar Vario EL III analytical instrument. The magnetic data of the powdered samples of **1**·MeOH·CH_2Cl_2 and **2**·3MeOH were recorded on a SQUID magnetometer (SQUID-VSM, Quantum Design) under an external magnetic field (0.5 T) in the temperature range 2−300 K. The magnetic susceptibility data were corrected with ligands' diamagnetism by the tabulated Pascal's constants.

Synthesis of 2,4,6-Tris(2-picolylamino)-1,3,5-triazine (*o*-H_3tpat). A solution of cyanuric chloride (1.84 g, 10.0 mmol) in THF (50 mL) was slowly added to a solution of 2-(aminomethyl)-pyridine (3.57 g, 33.0 mmol) in THF (50 mL) in an ice−water bath. Triethylamine (NEt_3, 6.68 mL, 66.0 mmol) was then added at room temperature. The mixture was stirred at 80 °C, and the reaction was monitored by TLC. The reaction was completed in approximately 48 h. After cooling to room temperature, the reaction solvent was removed under reduced pressure. The residue was extracted with an aqueous solution of potassium carbonate (aq. K_2CO_3, 4 equiv.) and dichloromethane (2 × 50 mL) followed by H_2O/CH_2Cl_2. The organic extracts were combined and dried with anhydrous $MgSO_4$. The pure product was obtained by recrystallization from MeOH/H_2O. Yield: 83% (3.23 g, 8.32 mmol). ^{1}H NMR (300 MHz, DMSO-d_6): δ 8.43 (br, d, J = 17 Hz, 3H), 7.63 (br, d, J = 50 Hz, 3H), 7.27−7.09 (br, m, 9H), 4.46 (br, d, J = 41 Hz, 6H) ppm. ^{13}C{^{1}H} NMR (75.5 MHz, DMSO-d_6): δ 166.18, 160.01, 148.77, 136.73,136.53, 121.91, 121.15, 120.94, 45.59, 45.42 ppm. IR (KBr pellet): 3400, 3257, 3214, 3058, 3011, 2975, 2933, 1623, 1569, 1521, 1479, 1437, 1341, 1252, 1222, 1174, 1096, 1048, 1000, 941, 898, 839, 815, 755, 683, 635, 611, 569, 510, 462 cm^{-1}. MS (MALDI-TOF): m/z = 400.08 [M]$^+$. Anal. calcd for $C_{12}H_{13}N_3$: C, 63.14; H, 5.30; N, 31.50%. Found: C, 63.02; H, 5.27; N, 31.65%. Colorless crystals suitable for X-ray diffraction analysis were obtained from MeOH/Et_2O (form **I**, triangle-shaped) or CH_2Cl_2/Et_2O (form **II**, block-shaped) at room temperature.

Synthesis of [Cu_3Cl_5(*o*-H_2tpat)(H_2O)]·MeOH·CH_2Cl_2 (1). A solution of $CuCl_2$ (28.7 mg, 2.1 × 10^{-1} mmol) in MeOH (5 mL) was carefully layered on top of a mixture of MeOH−CH_2Cl_2 (6 mL, 1:1 v/v, middle), and a solution of *o*-H_3tpat (19.9 mg, 5.0 × 10^{-2} mmol) in CH_2Cl_2 (5 mL, bottom) at room temperature. The solution was allowed to stand for approximately 4 weeks, resulting in the formation of green-colored crystals. Yield 76% (34.6 mg, 3.8 × 10^{-2} mmol). IR (KBr pellet): 3322, 3112, 3035, 1658, 1593, 1569, 1485, 1449, 1425, 1371, 1287, 1222, 1156, 1108, 1036, 893, 767, 719, 683, 653, 581, 540, 473, 420 cm^{-1}. Anal. calcd for $C_{21}H_{22}Cl_5Cu_3N_9O$: C, 32.16; H, 2.83; N, 16.07%. Found: C, 32.05; H, 3.31; N, 15.60%.

Synthesis of [Cu_2(*o*-H_2tpat)(H_2O)(MeOH)(NO_3)$_2$]-(NO_3)·3MeOH (2). Method 1. A solution of Cu(NO_3)$_2$·2.5H_2O (47.6 mg, 2.0 × 10^{-1} mmol) in MeOH (5 mL) was carefully layered on top of THF (6 mL, middle), and a solution of *o*-H_3tpat (20.0 mg, 5.0 × 10^{-2} mmol) in CH_2Cl_2 (5 mL, bottom) at room temperature. The solution was allowed to stand for approximately 2 weeks, resulting in the formation of deep-green crystals of **2**·3MeOH. Yield 76% (33.0 mg, 3.8 × 10^{-2} mmol). **Method 2.** A sample of Cu(NO_3)$_2$·2.5H_2O (47.6 mg, 2.0 × 10^{-1} mmol) and a sample of *o*-H_3tpat (20.0 mg, 5.0 × 10^{-2} mmol) were dissolved in DMF/MeOH mixture (7 mL, 2:5 v/v). The resulting solution was placed at the bottom of a test tube. Upon the solution were then successively layered MeOH (5 mL) and ethyl ether (10 mL). The solvents were allowed to diffuse slowly over 4 weeks at room temperature, resulting in the formation of deep-green crystals. Yield 60% (25.8 mg, 3.0 × 10^{-2} mmol). IR (KBr pellet): 3262, 3071, 3028, 2927, 2867, 1766, 1605, 1569, 1527, 1491, 1383, 1294, 1216, 1156, 1108, 1060, 1030, 982, 826, 767, 725, 683, 653, 551, 467, 432 cm^{-1}. Anal. calcd for $C_{22}H_{26}Cu_2N_{12}O_{11}$·2.5$H_2O$: C, 32.76; H, 3.87; N, 20.84%. Found: C, 32.31; H, 3.53; N, 21.32%.

X-ray Crystallography. Single-crystal X-ray diffraction analysis was performed by using a Bruker Smart CCD diffractometer equipped with graphite monochromatized Mo Kα radiation (λ = 0.71073 Å). Intensity data were collected at 296(2) K within the limits of 2.69° ≤ θ

dx.doi.org/10.1021/ic3016854 | *Inorg. Chem.* 2012, 51, 12360−12371

Table 1. Crystallographic Data for *o*-H_3tpat (Form I and Form II), 1, and 2

compounds	*o*-H_3tpat form I	*o*-H_3tpat form II	1	2
empirical formula	$C_{21}H_{21}N_9$	$C_{21}H_{21}N_9$	$C_{23}H_{28}Cl_7Cu_3N_9O_2$	$C_{25}H_{38}Cu_2N_{12}O_{14}$
M_w	399.47	399.47	901.31	857.75
crystal system	orthorhombic	triclinic	triclinic	monoclinic
space group	$Pna2_1$	$P\bar{1}$	$P\bar{1}$	$P2_1/c$
a (Å)	16.1737(19)	9.6725(3)	7.5069(4)	10.5146(12)
b (Å)	8.2290(9)	10.2291(3)	12.5901(7)	25.643(3)
c (Å)	15.1638(16)	11.6416(3)	16.6286(9)	13.6739(16)
α (deg)	90	111.9670(10)	88.738(3)	90
β (deg)	90	92.7320(10)	84.968(4)	107.448(7)
γ (deg)	90	111.5810(10)	85.381(3)	90
V (Å^3)	2018.2(4)	970.13(5)	1560.29(15)	3517.2(7)
Z	4	2	2	4
T (K)	296(2)	296(2)	296(2)	296(2)
λ (Å)	0.71073	0.71073	0.71073	0.71073
D_{calc} (g cm^{-3})	1.315	1.368	1.918	1.620
μ (mm^{-1})	0.085	0.089	2.667	1.292
F_{000}	840	420	902	1768
GOF	1.028	0.816	1.003	1.054
$R_1{}^a$ ($I > 2\sigma(I)$)	0.0333	0.0370	0.0620	0.0614
$wR_2{}^b$ ($I > 2\sigma(I)$)	0.0705	0.0919	0.1476	0.1645
$R_1{}^a$ (all data)	0.0420	0.0543	0.1215	0.0980
$wR_2{}^b$ (all data)	0.0739	0.1049	0.1862	0.1920
$\Delta\rho_{max}/\Delta\rho_{min}$ (e Å^{-3})	0.151/−0.167	0.158/−0.209	0.716/−1.142	1.351/−0.609

$^a R_1 = \sum||F_o|-|F_c||/\sum|F_o|$. $^b wR_2 = \{\sum[w(F_o^2 - F_c^2)^2]/\sum[w(F_o^2)^2]\}^{1/2}$.

$\leq 25.00°$ and $1.93° \leq \theta \leq 25.05°$ for the form **I** and form **II** of the *o*-H_3tpat ligand, respectively, and $1.23° \leq \theta \leq 25.12°$ for **1** and $1.59° \leq \theta \leq 25.14°$ for **2**. Starting models for structure refinement were solved by direct methods using *SHELXS-97*,[25] and the structural data were refined by full-matrix least-squares methods on F^2 using the *WINGX*[26] and *SHELX-97*[25] program packages. Anisotropical thermal factors were assigned to non-hydrogen atoms. Carbon- and triazine nitrogen-bound hydrogen atoms in **1** and **2** were assigned by geometrical calculation and refined as a riding mode. Oxygen and secondary amine nitrogen-bound hydrogen atoms in *o*-H_3tpat form **I** and form **II** as well as **2** were structurally evident in difference Fourier maps. Isotropic displacement parameters of all hydrogen atoms were derived from the parent atoms. Experimental details for X-ray data collection and the refinements are summarized in Table 1.

Computational Method. Geometry optimizations of the all-amino (conformers **A** and **B**) and all-imino (conformer **C**) resonative tautomers of *o*-H_3tpat have been carried out using the B3LYP functional theory incorporating the Becke's three parameter exchange functional (B3)[27] with Lee, Yang, and Parr (LYP) correlation functional[28] employing the *Gaussian 03* program.[29] The internally stored 6-31G* basis set was employed.[30] Stationary point geometries thus obtained were characterized as local minima on the potential energy surface since all the frequencies of normal vibrations for these structures turn out to be real.

RESULTS AND DISCUSSION

Synthesis and Structural Properties of *o*-H_3tpat. The tripodal ligand, *o*-H_3tpat, has been prepared in moderate yield by reaction of cyanuric chloride with 2-picolylamine using triethylamine in THF at 80 °C for 48 h. The molecular structure has been characterized by spectroscopic analysis undoubtedly. It is noted that the ^{1}H NMR spectrum of *o*-H_3tpat in DMSO-d_6 at room temperature shows broadened proton resonances (Figure S1, Supporting Information). This reasonably hints that there may be several conformation forms for *o*-H_3tpat in the solution state, and these configuration isomers interconvert with each other in a rate closed to the NMR time scale. However, an a priori exclusion of some conformers is not evident and the preference of the amino- or imino-form does not confirm conclusively.[21] Fortunately, two condensed polymorph forms **I** and **II** of *o*-H_3tpat have been obtained as colorless crystals suitable for X-ray structural determination, providing a definitive proof of ligand conformation in the solid-state.

The *o*-H_3tpat form **I**, obtained as triangle-shaped crystals by layering ethyl ether on top of a solution of *o*-H_3tpat in methanol, belongs to the orthorhombic space group $Pna2_1$ and demonstrates a molecular structure in an all-amino form, as evidenced by the $N_{outer}-C_{triazine}$ bond distances of 1.354(3)−1.358(3) Å and the $N_{inner}-C_{triazine}$ bond distances of 1.336(3)−1.352(3) Å (Table 2). The *o*-H_3tpat ligand, from the geometric isomerism point of view, has an asymmetric configured aminotriazine core attaching to three freely rotating pyridyl groups in a *cis*−*trans*−*trans* manner (Figure 1a).[31] Intramolecular C−H···π interactions (C···C/N, 3.91−4.44 Å) are observed between the two *cis*-orientated pyridyl groups that have a dihedral angle of 64.7°. Each *o*-H_3tpat ligand contacts to six neighbors through mainly six classic stronger $N_{outer}-H\cdots N_{py}$ hydrogen bonds (N···N, 2.932(2)−3.185(2) Å, Figure 1b and Table 3) and further two pertinent weak $C-H\cdots N_{inner}$ hydrogen bonds (C···N, 3.549(3) Å), leading to a three-dimensional supramolcular assembly (Figure S4, Supporting Information).

The *o*-H_3tpat form **II**, obtained as rectangle-shaped crystals from a solvent system of dichloromethane/ethyl ether, crystallizes in the triclinic space group $P\bar{1}$ and has a molecular structure in an all-amino form with an asymmetric configured aminotriazine core (Figure 2a). The $N_{outer}-C_{triazine}$ and the $N_{inner}-C_{triazine}$ bond distances are in the range 1.345(2)−1.356(2) Å and 1.336(2)−1.352(2) Å, respectively (Table 2). Two *o*-H_3tpat molecules form a dimeric assembly via DADA−ADAD quadruple $N_{outer}-H\cdots N_{inner}$ and $N_{outer}-H\cdots N_{py}$ hydro-

dx.doi.org/10.1021/ic3016854 | *Inorg. Chem.* 2012, 51, 12360−12371

Table 2. Selected Bond Lengths (Å) and Angles (deg) for the Aminotriazine Moiety of the *o*-H_3tpat Ligand in Form I and Form II and of the *o*-H_2tpat$^-$ Ligand in Complexes 1 and 2

compds	*o*-H_3tpat form I	*o*-H_3tpat form II	1	2
N1–C1	1.345(3)	1.340(2)	1.360(10)	1.380(8)
N1–C2	1.352(3)	1.350(2)	1.372(10)	1.381(7)
N2–C2	1.336(3)	1.347(2)	1.331(10)	1.342(7)
N2–C3	1.348(3)	1.345(2)	1.354(10)	1.331(7)
N3–C3	1.348(3)	1.336(2)	1.369(10)	1.337(7)
N3–C1	1.346(2)	1.352(2)	1.383(10)	1.331(7)
N4–C1	1.354(3)	1.345(2)	1.291(10)	1.318(7)
N4–C4	1.453(3)	1.443(2)	1.480(11)	1.451(8)
N5–C2	1.358(3)	1.346(2)	1.314(10)	1.313(7)
N5–C10	1.464(3)	1.453(2)	1.460(10)	1.468(7)
N6–C3	1.355(3)	1.356(2)	1.298(10)	1.379(7)
N6–C16	1.460(3)	1.440(2)	1.456(10)	1.477(7)
C1–N4–C4	123.17(17)	124.35(14)	114.8(7)	117.2(5)
C2–N5–C10	122.56(17)	123.39(13)	115.4(7)	113.6(5)
C3–N6–C16	123.06(17)	122.71(13)	118.2(6)	118.4(5)

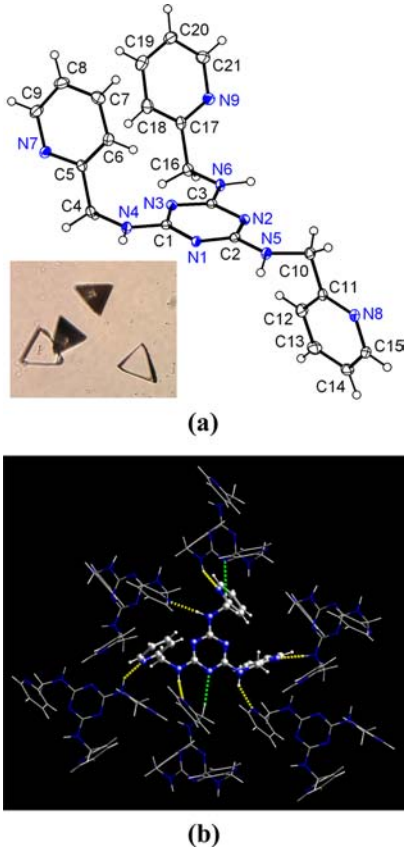

Figure 1. Molecular structure of *o*-H_3tpat form **I**. (a) ORTEP depiction together with the photograph of the triangle-shaped single crystals. Displacement ellipsoids are drawn at the 30% probability level. (b) Representation of the environment of one *o*-H_3tpat molecule, which was surrounded by six neighboring *o*-H_3tpat molecules through pertinent N_{outer}–H···N_{py} (yellow dashed lines) and C–H···N_{inner} hydrogen bonds (green dashed lines).

gen bonds (N···N, 2.992(2)–3.032(2) Å, Figure 2b and Table 3), which leads to an extended supramolcular assembly through pertinent weaker C–H···N_{py} hydrogen bonds (C···N, 3.377(3) Å, Figure S5, Supporting Information) and C–H···π interactions (C···C/N, 3.49–4.41 Å).

Table 3. Hydrogen Bonding Parameters for *o*-H_3tpat Form I and Form II

D–H···A	D–H (Å)	H···A (Å)	D···A (Å)	D–H···A (deg)	symmetry code
form **I**					
N4–H101···N8	1.00	2.07	2.932(2)	143	$^1/_2 - x$, $^1/_2 + y$, $-^1/_2 + z$
N5–H102···N9	0.99	2.30	3.185(2)	148	$^1/_2 + x$, $^1/_2 - y$, z
N6–H103···N7	0.99	2.02	3.003(3)	176	$-x$, $1 - y$, $^1/_2 + z$
C16–H16B···N1	0.97	2.59	3.549(3)	172	$-^1/_2 + x$, $^1/_2 - y$, z
form **II**					
N5–H102···N2	0.97	2.08	3.032(2)	166	$1 - x$, $1 - y$, $1 - z$
N6–H103···N8	0.94	2.07	2.992(2)	164	$1 - x$, $1 - y$, $1 - z$
C4–H4A···N9	0.97	2.70	3.377	127	x, $1 + y$, z

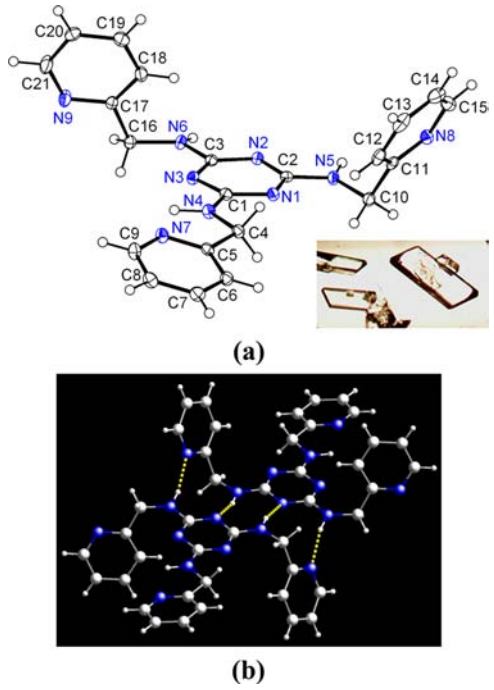

Figure 2. Molecular structure of *o*-H_3tpat form **II**. (a) ORTEP depiction together with the photograph of the rectangle-shaped single crystals. Displacement ellipsoids are drawn at the 30% probability level. (b) Representation of the dimeric assembly of *o*-H_3tpat arising from the DADA–ADAD quadruple hydrogen bonds.

Preparation of Copper(II) Complexes. Slow diffusion of a methanol solution of $CuCl_2$ into a dichloromethane solution of as-synthesized *o*-H_3tpat with a mixture of MeOH and CH_2Cl_2 as buffer at room temperature has yielded green crystalline products of $[Cu_3Cl_5(o\text{-}H_2tpat)(H_2O)]\cdot MeOH\cdot CH_2Cl_2$ (**1**), whereas $[Cu_2(o\text{-}H_2tpat)(H_2O)(MeOH)(NO_3)_2](NO_3)\cdot 3MeOH$ (**2**) has been obtained as deep-green crystals from the diffusion of a methanol solution of $Cu(NO_3)_2\cdot 2.5H_2O$ into a dichloromethane solution of *o*-H_3tpat with THF as buffer. Alternatively, **2** has also been prepared

dx.doi.org/10.1021/ic3016854 | *Inorg. Chem.* 2012, 51, 12360–12371

from the reaction system of $Cu(NO_3)_2{\cdot}2.5H_2O$ and *o*-H_3tpat in DMF:MeOH mixture at room temperature.

Crystal Structure of $[Cu_3Cl_5(o\text{-}H_2tpat)(H_2O)]{\cdot}MeOH{\cdot}CH_2Cl_2$ (1). A single-crystal X-ray diffraction analysis of **1** reveals that the asymmetric unit contains three crystallographically independent copper(II) ions together with five chloride monoanions, one monoanionic *o*-H_2tpat^- ligand, and one aqua ligand to complete the coordinative-motif, as well as one lattice methanol and one lattice dichloromethane molecule (Figure 3). Each unique copper ion has a distinctive

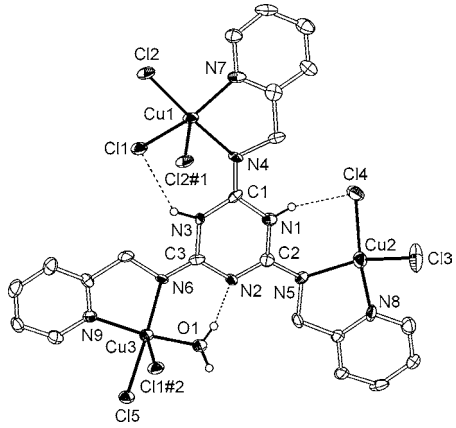

Figure 3. ORTEP depiction showing the coordination environment around the metal ions and the coordination mode of *o*-H_2tpat^- ligand with selected numbering scheme in **2**. Pertinent N_{inner}–H···Cl and O_{aqua}–H···N_{inner} hydrogen bonds are represented by dotted lines. The carbon-bound hydrogen atoms are omitted for clarity. Displacement ellipsoids are drawn at the 50% probability level. Symmetry transformations used to generate equivalent atoms: #1, $-x + 2$, $-y + 1$, $-z$; #2, $x - 1$, y, z.

coordination environment: Cu(1) has a N_2Cl_3-coordination sphere made of an iminopyridyl chelating group and three μ-chloro ligands; Cu(2) has a N_2Cl_2-coordination sphere made of an iminopyridyl chelating group and two terminal chloro ligands; and Cu(3) has a N_2OCl_2-coordination sphere made of an iminopyridyl chelating group and one aqua, one μ-chloro, and one terminal chloro ligands. Both of the two pentacoordinated copper ions, Cu(1) and Cu(3), exhibit distorted square pyramidal geometries with τ values of 0.38 and 0.18, respectively.[32] The tetracoordinated Cu(2) ion shows a highly distorted square planar geometry with the bond angles ranged from 83.6(3)° to 146.0(2)°. It is noted that the tripodal ligand herein, for achieving charge-neutralization, is found to be monoanion, *o*-H_2tpat^-. Meanwhile, the N_{outer}–$C_{triazine}$ bond distances of 1.291(10)–1.314(10) Å and the N_{inner}–$C_{triazine}$ bond distances of 1.331(10)–1.383(10) Å are, respectively, somewhat shorter and longer than those in both *o*-H_3tpat form **I** and form **II** (Table 2). In addition, the sum of the bond angles of nearly 360° surrounding the out-of-ring nitrogens indicates that all the out-of-ring nitrogens are of approximately sp^2 configuration (Table S1, Supporting Information).[19] These observations clearly indicate that the monoanionic *o*-H_2tpat^- ligand herein exists in an all-imino resonative structure with two protons bonded to two of the three triazine nitrogens (N_{inner}). On the other hand, the *o*-H_2tpat^- ligand has a propeller configuration in geometry and adopts a tris-bidentate chelating mode through its pyridyl and out-of-ring imino nitrogen atoms toward three copper ions (Figure 3), forming a fundamental trimetallic repeating unit $\{Cu_3Cl_5(o\text{-}H_2tpat)(H_2O)\}$. Pertinent N_{inner}–H···Cl hydrogen bonds between the protonated triazine hydrogens and chloro ligands (N···Cl, 3.084(7)–3.112(7) Å, Table 4) and O_{aqua}–H···N_{inner} hydrogen bonds between the aqua hydrogen and the unprotonated triazine nitrogen (O···N, 2.591(9) Å) are observed within the trimetallic entity.

The trimetallic repeating unit $\{Cu_3Cl_5(o\text{-}H_2tpat)(H_2O)\}$ interacts with three units through the connection of further coordination-bonds between the copper ions (Cu(1) and Cu(3)) and the chloro anions (Cl(1) and Cl(2)) from neighboring units and vice versa to form a one-dimensional tape-like coordination-chain structure running along the crystallographic *a* axis (Figure 4a). The chain-forming Cu–Cl bonds are at the apical positions of the pentacoordinated copper ions and have distances of 2.723(2)–2.770(2) Å, significantly exhibiting bond approximately 0.5 Å longer than the basal Cu–Cl bonds (2.267(2)–2.278(2) Å), indicating only loose association of the trimetallic repeating units. Lattice methanol molecules make contacts with the coordination-chains through $O_{methanol}$–H···Cl hydrogen-bonding interactions

Table 4. Hydrogen Bonding Parameters for 1 and 2

D–H···A	D–H (Å)	H···A (Å)	D···A (Å)	D–H···A (deg)	symmetry code
1					
N1–H101···Cl4	0.86	2.36	3.112(7)	146	
N3–H102···Cl1	0.86	2.45	3.084(7)	132	
O1–H103···N2	0.83	1.78	2.591(9)	165	$x + 1, y, z$
O1–H104···Cl5	0.82	2.25	3.047(6)	162	$-x + 2, -y, -z$
O2–H105···Cl2	0.85	2.74	3.189(8)	114	$-x + 2, -y + 1, -z$
2					
N1–H101···O4	0.86	1.99	2.762(6)	149	
N6–H102···O7	0.89	2.03	2.906(8)	171	
O10–H103···O7	0.84	2.56	3.032(7)	117	
O10–H103···N3	0.84	1.92	2.663(6)	148	
O10–H104···O23	0.84	1.86	2.707(7)	177	$x, -y + {}^1/_2, z + {}^1/_2$
O22–H105···O25	0.86	1.90	2.672(10)	147	
O23–H106···O7	0.86	2.50	3.042(7)	122	$x, -y + {}^1/_2, z - {}^1/_2$
O23–H106···O9	0.86	1.98	2.821(7)	166	$x, -y + {}^1/_2, z - {}^1/_2$
O24–H107···O2	0.90	1.93	2.775(8)	156	
O25–H108···O24	0.89	2.05	2.746(12)	134	$1 + x, y, z$

dx.doi.org/10.1021/ic3016854 | *Inorg. Chem.* 2012, 51, 12360–12371

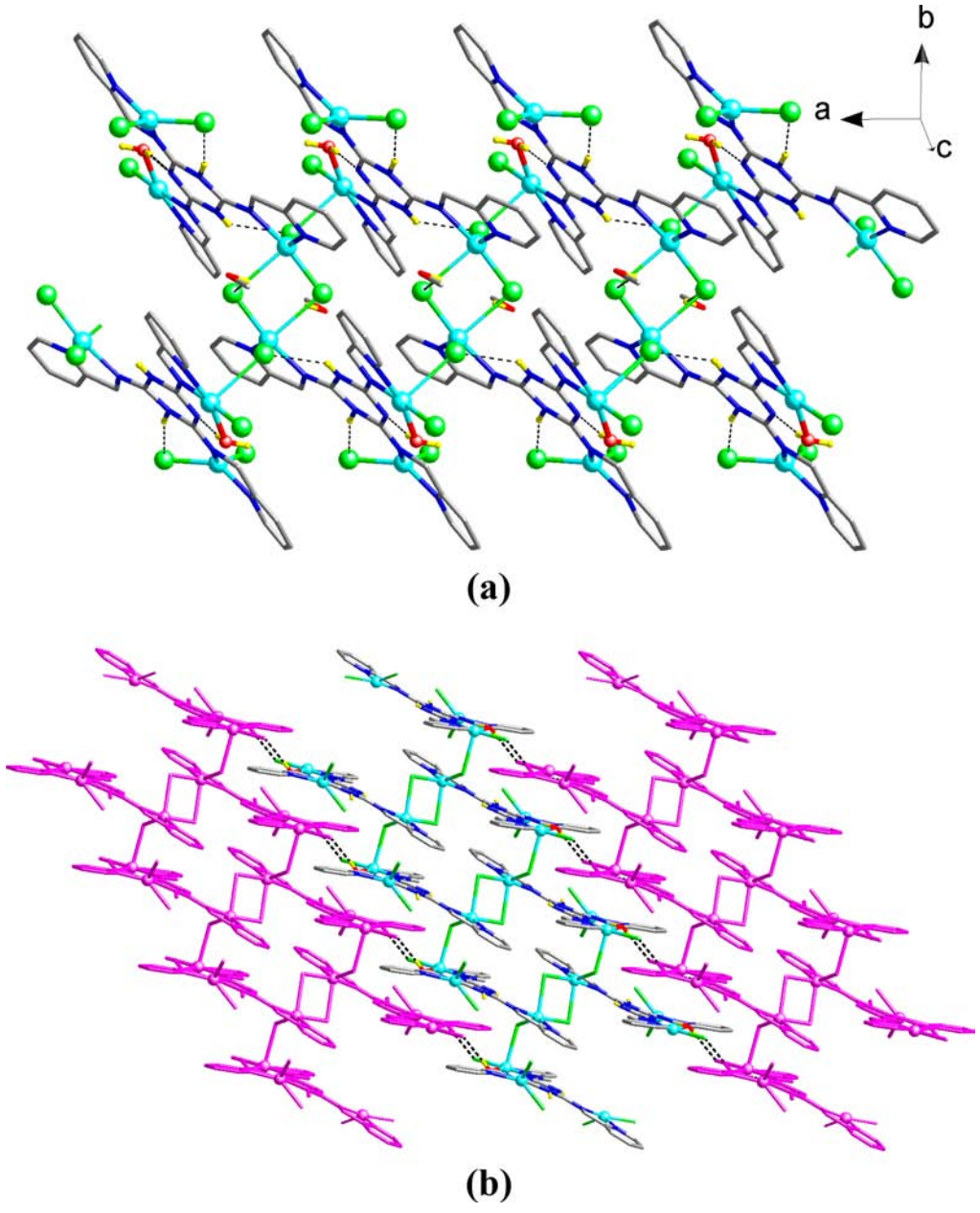

Figure 4. (a) Representation of the one-dimensional tape-like coordination-chain structure in **1**. Carbon-bound hydrogen atoms and lattice dichloromethane molecules are omitted for clarity. Color scheme: cyan, Cu; green, Cl; red, O; blue, N; gray, C; yellow, H. (b) Representation of chain-to-chain O_{aqua}–H···Cl hydrogen-bonding interactions assisted supramolecular sheet in **1** view down the crystallographic *c* axis.

(O···Cl, 3.189(8) Å) between the hydroxyl hydrogens and the μ-chloro ligands of the $Cu_2(\mu\text{-}Cl)_2$ rhombs. On the other hand, there are also chain-to-chain O_{aqua}–H···Cl hydrogen-bonding interactions (O···Cl, 3.047(6) Å) between the coordination aqua hydrogens in one chain and the terminal-chloro ligands in neighboring chains, leading to a sheeted supramolecular array extended in the *ab* plane (Figure 4b).

Crystal Structure of $[Cu_2(o\text{-}H_2tpat)(H_2O)(MeOH)(NO_3)_2](NO_3)\cdot 3MeOH$ (2). A single-crystal X-ray diffraction analysis of **2** reveals that the asymmetric unit contains two crystallographically independent copper(II) ions, three nitrate anions, one monoanionic *o*-H_2tpat^- ligand, one water molecule, and four methanol molecules (Figure 5). The designed tripodal ligand in **2** is also a monoanion of *o*-H_2tpat^- in saturating the requirement of charge-neutralization. Two of the three N_{outer}–$C_{triazine}$ bonds show distances of 1.313(7) and 1.318(7) Å (Table 2), significantly indicating the imino N–C double-bond character. This is further supported by the sum of the bond angles of nearly 360° surrounding the out-of-ring nitrogens (Table S1, Supporting Information). Comparatively, the third N_{outer}–$C_{triazine}$ bond distance is 1.379(7) Å and the sum of the bond angles surrounding the N_{outer} atom is approximately 323°, being an amino N–C single-bond. Therefore, the *o*-H_2tpat^- ligand herein demonstrates an amino–imino–imino resonative structure in which only one of the three triazine nitrogens is protonated. From the geometric isomerism point of view, the *o*-H_2tpat^- ligand has a *syn–anti* configuration and coordinates to three copper ions in a tris-chelating manner of its two iminopyridyl and one aminopyridyl moieties (Figure 5). There are pertinent N_{inner}–H···$O_{nitrato}$ hydrogen bonds between the protonated triazine hydrogen and the coordinated nitrato oxygen (N···O, 2.762(6) Å, Table 4) and O_{aqua}–H···N_{inner}

dx.doi.org/10.1021/ic3016854 | *Inorg. Chem.* 2012, 51, 12360–12371

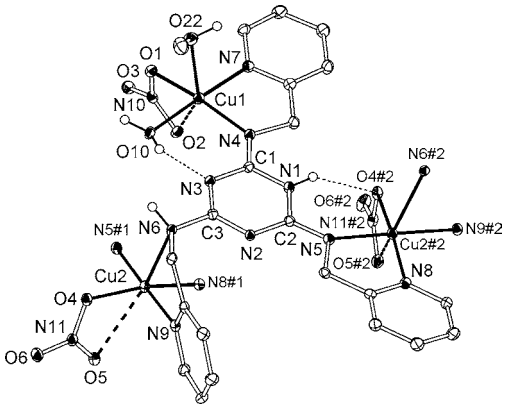

Figure 5. ORTEP depiction showing the coordination environment around the copper ions and the trimetallic coordination mode of *o*-H_2tpat^- ligand with selected numbering scheme in **2**. Semicoordinate Cu−$O_{nitrato}$ bonds are shown as dashed lines. Pertinent O_{aqua}−H···N_{inner} and N_{inner}−H···$O_{nitrato}$ hydrogen bonds are represented by dotted lines. The carbon-bound hydrogen atoms and uncoordination nitrate counteranions are omitted for clarity. Displacement ellipsoids are drawn at the 15% probability level. Symmetry transformations used to generate equivalent atoms: #1, $x, -y + {}^3/_2, z - {}^1/_2$; #2, $x, -y + {}^3/_2, z + {}^1/_2$.

hydrogen bonds between the aqua hydrogen and the unprotonated triazine nitrogen (O···N, 2.663(6) Å).

On the other hand, both the two crystallographically distinct copper ions are pentacoordinated but in different environments. While Cu(1) has a N_2O_3-coordination sphere comprised of an iminopyridyl chelating group, one aqua and one monodentate nitrato ligands, and one methanol molecule, Cu(2) is in a N_4O-coordination sphere made of an iminopyridyl and an aminopyridyl chelating groups of two different *o*-H_2tpat^- ligands and one monodentate nitrato ligand. Both Cu(1) and Cu(2) show distorted square pyramidal geometries with τ values of 0.20 and 0.14, respectively.[32] The apical Cu−$O_{methanol}$ of 2.249(5) Å in Cu(1) and Cu−N_{outer} of 2.459(5) Å in Cu(2) bond lengths are significantly longer than these (Cu−O, 1.930(4)−2.054(4) Å; Cu−N, 1.976(5)−2.024(5) Å) in the basal plane due to the Jahn−Teller distortion. However, when the long Cu···$O_{nitrato}$ bonds (Cu1···O2, 2.572 Å and Cu2···O5, 2.587 Å) are taken into consideration, the coordination environments of Cu(1) and Cu(2) can also be described as distorted octahedral geometries.

Compound **2** has a belt-like coordination chain structure running along the crystallographic *c* axis (Figure 6a). Intrachain $\pi-\pi$ interactions showing a centroid···centroid distance of 3.494 Å are observed between the triazine core of one *o*-H_2tpat^- ligand and the pyridine ring of next one. The coordination chain structure in **2** is positively charged. Charge compensation is achieved through one further nitrate counteranion per formula. Multiform hydrogen-bonding interactions are observed between the nitrate counteranion and the coordination chain and a further lattice methanol molecule (N/O···O, 2.707(7)−3.042(7) Å, Figure S6, Supporting Information, and Table 4). Extensive packing reveals that the coordination chains communicate with each other through a sequence of hydrogen-bonding interactions that form from the ligated methanol molecules in one chain to the lattice methanol molecules and following to the coordinated nitrato ligands in the next chain ($O_{methanol}$···$O_{methanol/nitrato}$, 2.672(10)−2.775(8) Å, Figure 6b and Table 4).

Ligand Conformation. The free *o*-H_3tpat ligand exhibits two different macroscopic crystal shapes arose from different crystallization conditions, which directly refer to the ligand conformations. In order to get more information about the ligand conformations, electronic structure calculations based on the all-amino tautomeric form **I** and form **II** of the *o*-H_3tpat ligand (conformers **A** and **B**) and, in comparison, the all-imino resonative tautomer (conformer **C**) are therefore made. B3LYP/6-31G** theory level optimized geometries in the ground state are shown in Figure 7 and the selected bond distances and angles are reported in Table S2, Supporting Information. As calculations, the optimized all-amino tautomeric conformers **A** and **B** exhibits more negative value of minima stabilization energy than that showed by the all-imino tautomeric conformer **C**, indicating that the all-amino form of the *o*-H_3tpat ligand is the thermodynamic stable tautomer. In addition, for the two all-amino resonative structures, conformer **B** is relatively stable compared with conformer **A**. However, the energy difference among the three conformers is very small (<0.211 eV); therefore, it is reasonable that they are easily interconverted with each other in the solution state, even under mild conditions, as observed in the room temperature proton NMR spectrum showing broadened peak signals (Figure S1, Supporting Information).

On the other hand, the designed tripodal ligand in both **1** and **2** serves as a monoanion, *o*-H_2tpat^-, which shows a propeller-configured all-imino resonative structure in **1** and a *syn*−*anti*-configured amino−imino−imino resonative structure in **2**. These results significantly indicate that the *o*-H_3tpat ligand seems to prefer all-amino tautomeric conformations in the free ligand, as the computational results, and then it would interconvert into an imino-based resonative structure upon both electronic and geometric isomerization when complexating with metal ions. In the literature, there are also metal−organic architectures exhibiting ligand tautomerism upon coordination/chelation of a metal ion.[33] However, for such an aminotriazine-derived ligand with distinctively resonative structure, the effects of the solvents (the polarity and the hydrogen bond ability etc.) and the anions become more noticeable in dominating conformational preferences of the ligand, leading to a variety of coordination networks.[20,23] Additionally, the position of the pyridine-N donors seems to have a profound effect upon ligand tautomerism. In our previous work,[24] the coordination chemistry of the 2,4,6-tris(3-picolylamino)-1,3,5-triazine (*m*-H_3tpat) ligand, a positional isomer of *o*-H_3tpat, with Cu(II) and Co(II) ions has been studied. Within the structures, the *m*-H_3tpat ligand adopts an asymmetric-configured all-amino tautomeric conformation that is comparable with those showed by *o*-H_3tpat in **1** and **2**. This difference is reasonably attributed to the fact that the out-of-ring nitrogens in *o*-H_3tpat prefer to bind metal ions together with the 2-pyridine N donors but do not with the 3-pyridine N donors in *m*-H_3tpat. The chelating preference in coordination for *o*-H_3tpat might facilitate the occurrence of prototropic tautomerism, as observed in **1** and **2**.

Thermal Properties. Thermogravimetric (TG) analyses of **1** and **2** were performed under a nitrogen atmosphere in examining the thermal stabilities of those compounds (Figure S8, Supporting Information). The TG curve of **1** reveals that the lattice solvent molecules (MeOH and CH_2Cl_2) were lost between room temperature and 61 °C (found 6.6%, calcd. 6.9% for $[Cu_3Cl_5(o\text{-}H_2tpat)(H_2O)]\cdot{}^1/_2MeOH\cdot{}^1/_2CH_2Cl_2$), coordinated aqua ligands were released between 158−180 °C (found

dx.doi.org/10.1021/ic3016854 | *Inorg. Chem.* 2012, 51, 12360−12371

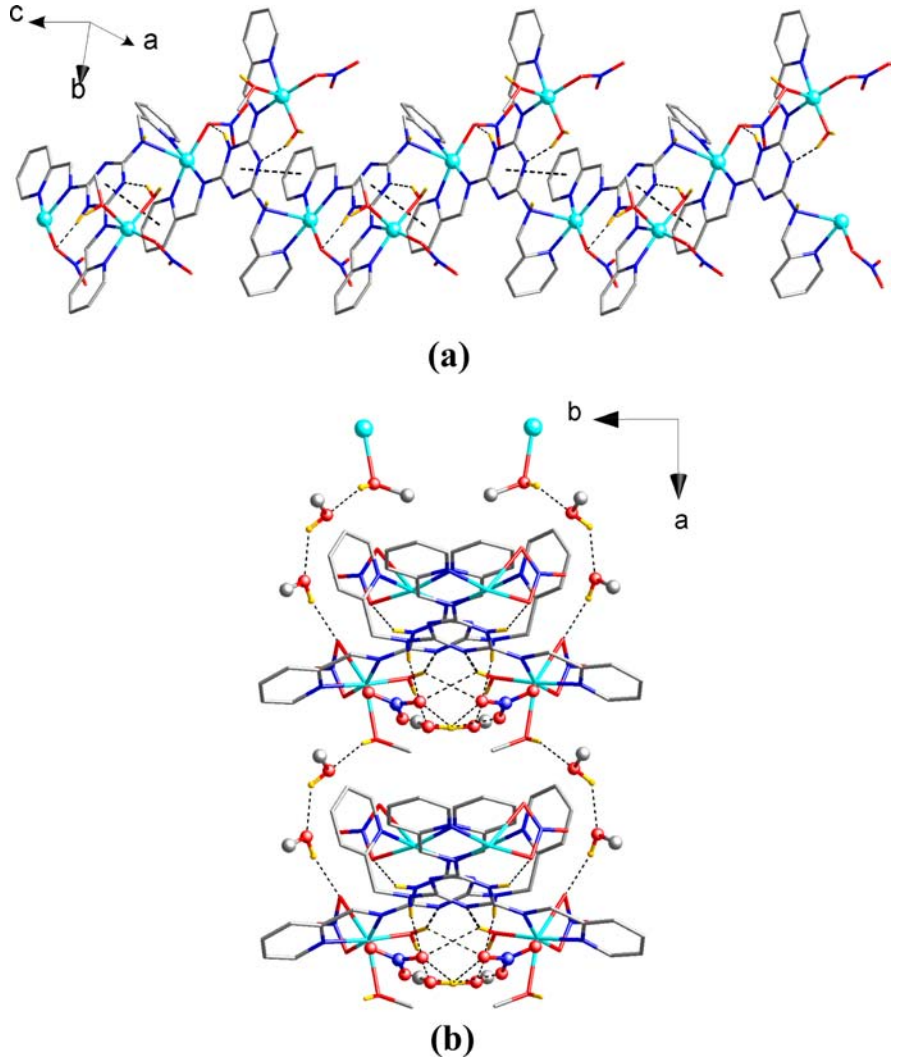

Figure 6. (a) Representation of the one-dimensional cationic belt-like coordination-chain structure in **2**. Carbon-bound hydrogen atoms, nitrate counteranions, and lattice methanol molecules are omitted for clarity. (b) Part of packing in **2** viewed down the crystallographic *c* axis, showing the heart-like hydrogen bonding nets formed between the coordination-chain and the lattice methanol molecules. Color scheme: cyan, Cu; red, O; blue, N; gray, C; yellow, H.

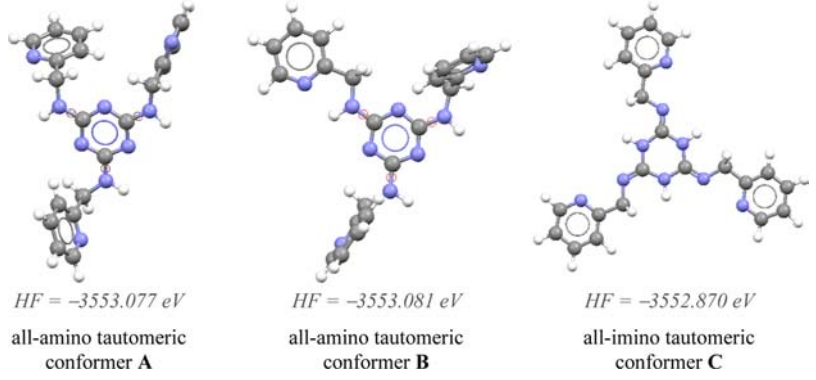

Figure 7. B3LYP/6-31G** optimized geometries of the all-amino (conformers **A** and **B**) and the all-imino (conformer **C**) tautomers of the *o*-H_3tpat ligand.

2.8%, calcd. 2.1%), and the solvent-free coordination-motif decomposed when the temperature was raised to approaching 210 °C. For **2**, the TG trace exhibits a gradual weight loss between room temperature and 156 °C, corresponding to the release of lattice methanol molecules (found 11.6%, calcd. 11.2%). This is followed by a small amount of weight loss between 156 and 165 °C, which corresponds to the loss of the ligating water and methanol molecules (found 6.1%, calcd. 5.9%). This agrees well with the X-ray crystallographic data. However, an abrupt weight loss occurs between 165−169 °C,

dx.doi.org/10.1021/ic3016854 | *Inorg. Chem.* 2012, 51, 12360−12371

indicating the decomposition of the solvent-free coordination-motif.

Magnetic Properties. Magnetic susceptibility data of a powdered sample of **1** was collected in the temperature range of 2−300 K (Figure 8). The experimental $\chi_M T$ value of 3.25

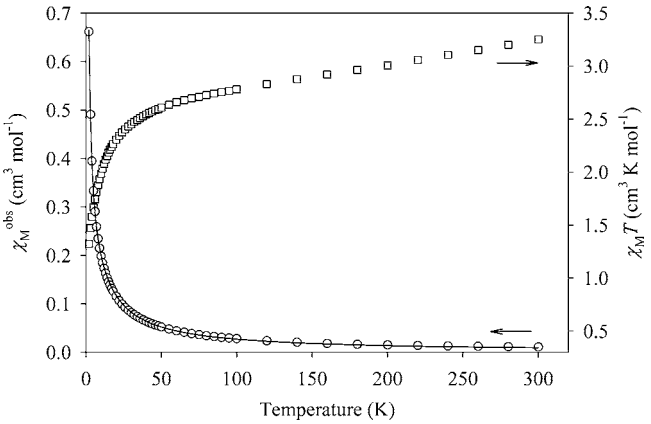

Figure 8. Plots of χ_M^{obs} (open circles) and $\chi_M T$ (open squares) versus temperature for **1**. The solid line is the best fit of the experimental data to the theoretical model.

cm^3 K mol^{-1} at 300 K is higher than the spin-only value of 2.25 cm^3 K mol^{-1} for a Cu(II)$_6$ system with g = 2. The $\chi_M T$ value decreases to 1.32 cm^3 K mol^{-1} as the temperature reaches 2 K, suggesting antiferromagnetic coupling is operative between the Cu(II) centers.

In the magnetic point of view, **1** is considered as repeated chains composed of infinite {Cu_6Cl_{10}} units (Scheme 2). Two

Scheme 2. 1 Considered As Repeated Chains Composed of Infinite {Cu_6Cl_{10}} Units

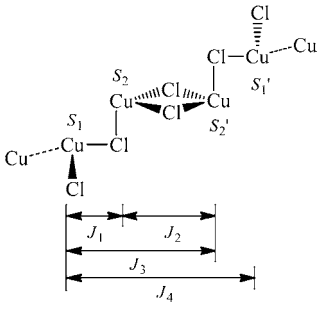

Cu centers are linked by two Cl$^-$ bridges to give a Cu_2Cl_2 square having a Cu···Cu distance of 3.661 Å. The Cu_2Cl_2 square is further connected to two Cu centers via two Cl$^-$ bridges to construct a stairway structure for which a distance of 4.211 Å between the outer and inner Cu sites is recorded. Two additional distant Cu centers are located at positions with the closest contact of 7.362 Å. Therefore, the hexanuclear unit can be further decomposed to one {$Cu(II)_4Cl_6$} and two magnetically isolated {$Cu(II)Cl_2$} subunits. The reduced magnetization study shows at 2 K it is saturated at ∼2.3 Nμ_B under 7 T, which suggests spin ground state (S_T = 1) and $g \approx$ 2.3 (Figure S9, Supporting Information). The result is consistent with the magnetic model in which an overall spin ground state is a combination of one singlet of the tetranuclear unit and two noninteracting doublets of the Cu(II) sites.

$$\chi_M^{obs} = \chi_M^{Cu4} + 2\chi_M^{Cu(s.o.)}$$

The 4J Hamiltonian is derived for the centrosymmetric Cu_4 system where J_1 and J_2 describe the nearest neighbor interactions between the outer and the inner centers, and two inner spins, respectively. J_3 is the coupling parameter for two next-nearest neighbor spins. J_4 describes the exchange constant between two outer spins. S_1 (S_1') and S_2 (S_2') represent the spins of the outer and inner Cu centers. Here, the g-factor is treated as a global parameter for simplicity.[34]

$$H = -2J_1(S_1 \cdot S_2 + S_1' \cdot S_2') - 2J_2(S_2 \cdot S_2') - 2J_3(S_1 \cdot S_2' + S_1' \cdot S_2) - 2J_4(S_1 \cdot S_1')$$

The best fit to the theoretical expression corresponds to g = 2.33, $2J_1$ = −5.6 cm^{-1}, $2J_2$ = −8.6 cm^{-1} and $2J_3$ = −4.1 cm^{-1} with J_4 held to zero. The agreement factor (R), which is defined as $\Sigma(\chi_M^{calcd} - \chi_M^{obs})^2 / \Sigma(\chi_M^{obs})^2$, is 9.8 × 10^{-5}. If interchain interactions (zJ') are considered,[35] the experimental data fitted to the modified expression give g = 2.33, $2J_1$ = −5.2 cm^{-1}, $2J_2$ = −8.5 cm^{-1} and $2J_3$ = −5.2 cm^{-1}, zJ' = 0.2 cm^{-1}, and R = 9.1 × 10^{-5} with J_4 held to zero.

$$\chi_M^{ic} = \chi_M / (1 - zJ'\chi_M / Ng^2\mu_B^2)$$

The weak interaction between two Cu centers is explained by the asymmetric Cl$^-$ bridges. For the inner Cu_2 units, the distances of Cu1−Cl2 and Cu1′−Cl2 are 2.267(2) and 2.723(2) Å, respectively. For the inner/outer dimers, they are 2.278(2) and 2.770(2) Å for Cu1−Cl1 and Cu3−Cl1, respectively. The long Cu···Cu distances also diminish overlap between the centers: 3.661 and 4.211 Å for Cu1−Cu1′ and Cu1−Cu3, respectively. It has been suggested that the Cu−X−Cu angle (Φ) plays a major role on the magnetic interaction.[36] The larger angles of ∠Cu−Cl−Cu than 90° for both the inner Cu_2 (93.92°) and the inner/outer (112.66°) pairs suggest the presence of the antiferromagnetic coupling.

It has been noted that the exchange constant (J) in the related systems shows a relationship with the Φ/R parameter, R being the longer Cu−Cl distance. For the central Cu_2 unit, the Φ/R value of 34.49°/Å refers to ∼ −5 cm^{-1} derived from the plot of 2J as a function of Φ/R. It is closely matched with the fitted result ($2J_2$ = −8.6 cm^{-1}). A value of ∼−80 cm^{-1} is expected for the inner/outer Cu_2 pair according to the Φ/R ratio of 40.67°/Å. The fitted result of −5.6 cm^{-1} for $2J_1$ in contrast shows the significant deviation. The weaker communication between Cu(1) and Cu(3) is rationalized by the coordination sites of the Cl$^-$. The bridging Cl$^-$ is situated at the apical position of these Cu(II) centers, which would shut down the antiferromagnetic mechanism to be in favor of ferromagnetic interactions if an angle of 90° is obtained. The Cu(3) site has a distorted square pyramidal geometry (τ = 0.18). The Cu(1) site possesses a (4 + 1) coordination geometry that is intermediate between capped tetrahedral and square pyramidal (τ = 0.38). In combination with the large angle of Cu−Cl−Cu, the distorted coordination geometry allows exchange of the $d_{x^2-y^2}$ spins to occur in some degree, resulting in the weak antiferromagnetic interaction.

The same sign of three J parameters causes the terminal centers to be magnetically frustrated with the next-nearest neighbor centers.[37] The inner Cu spins align in the antiparallel configuration to each other. They are, in addition, antiferromagnetic coupled to the outer centers. The approximately

dx.doi.org/10.1021/ic3016854 | Inorg. Chem. 2012, 51, 12360−12371

same magnitude of J_1 and J_3, but smaller than J_2, leads to the up spin at the terminal position and is energetically degenerated with the down spin. Consequently, it results in the singlet ground state for the Cu_4 unit (Scheme 3).

Scheme 3. Cu_4 Unit

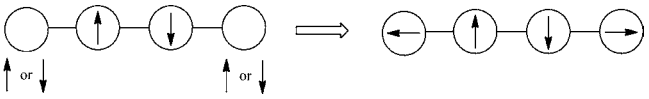

Magnetic susceptibility data of a powdered sample of **2** was collected in the temperature range of 2−300 K (Figure 9). The

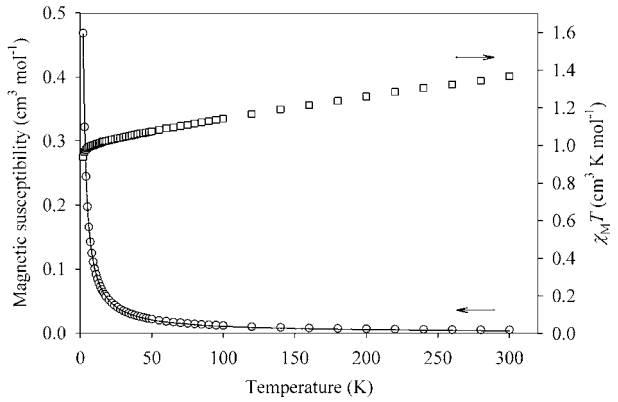

Figure 9. Plots of χ_M (open circles) and $\chi_M T$ (open squares) versus temperature for **2**. The solid line is the best fit of the experimental data to the theoretical model.

experimental $\chi_M T$ value of 1.37 cm^3 K mol^{-1} at 300 K is greater than the spin-only value of 0.75 cm^3 K mol^{-1} for a noninteracting Cu_2 system and slightly greater than the theoretical value of 1.00 cm^3 K mol^{-1} for a $S = 1$ system wherein the g value is set to 2 for both. The $\chi_M T$ value decreases as a function of the temperature to 0.94 cm^3 K mol^{-1} at 2 K. It reveals that the Cu(II) centers are antiferromagnetically interacted to reach a triplet spin ground state in **2**.

In the structure, each Cu center is intra- and intermolecularly coordinated by 2 to 3 N sites of the ligands to form 1-D chains that consist of belt-like structures with respect to the metal cores (Figure 10). The shortest distance between Cu(II) centers is 6.069 Å, followed by 7.417, 7.446, and 8.540 Å. The longest distance within a Cu_4 square plane is 9.535 Å from two diagonal Cu sites. The magnetic data of **2** is treated as an

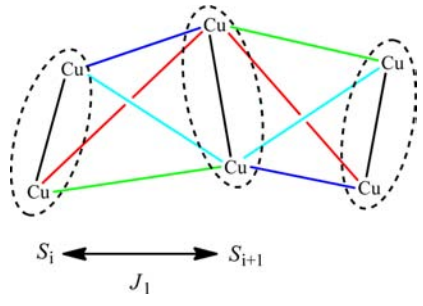

Figure 10. Schematic drawing of the magnetic interactions within **2**. The solid lines indicate the interactions between the $S = 1/2$ spins and their corresponding distances are 6.069 (black), 7.417 (blue), 7.446 (cyan), 8.540 (green), and 9.535 (red) Å.

infinite chain that composes of Cu_2 units antiferromagnetically coupled. No observable zero-field splitting is recorded in the reduced magnetization data. The triplet spin ground state is derived from the high-field and low-temperature measurement (Figure S10, Supporting Information).

The Hamiltonian for the isotropic antiferromagnetic chain is described as followed: $H = \sum (-2J_1 \cdot S_i \cdot S_{i+1})$.[38] Here, the g-factor is treated as a global parameter for simplicity. The best fit to the theoretical expression corresponds to $2J_1 = -0.2$ cm^{-1} and $g = 2.03$. The agreement factor (R) is 7.3×10^{-5}. The results suggest that the monoanionic o-H_2tpat$^-$ ligand is not a good spin mediator in the magnetic point of view. All spins are practically magnetic insulated.

CONCLUSION

In summary, the synthesis and X-ray characterization of a new aminotriazine-derived polypyridyl ligand, o-H_3tpat, and two copper(II)-based coordination polymers have been described. It is evidenced that slightly modifying the crystallization conditions can lead to different ligand conformations for o-H_3tpat in the solid state due to its distinctively resonative structure upon both electronic and geometric isomerization. On the other hand, the tripodal ligand in both the two copper(II)-based coordination chain structures appears to be a monoanionic form of o-H_2tpat$^-$, which adopts a propeller-configured all-imino resonative structure in **1** and a *syn*−*anti*-configured amino−imino−imino resonative structure in **2**. These results agree that the varied conformers of the resonative o-H_3tpat ligand can interconvert with each other through a possible prototropic tautomerism in the solution state and, consequently, self-adjusts its conformation to adapt a change in the self-assembly system in facilitating the formation of the most stable crystalline products. Magnetic studies reveal that every two Cu centers are antiferromagnetically coupled via the chloride bridges in **1**. The largest interaction occurs to the Cu_2Cl_2 subunits wherein two metal sites are of the shortest distance. For **2**, very weak antiferromagnetic interactions are observed between the Cu centers. Since the copper sites are coordinated to 1 or 2 o-H_2tpat$^-$ ligands within both coordination polymers, it is indicated by the weak magnetic interactions that the o-H_2tpat$^-$ ligand is a poor spin mediator. We anticipate that the use of the tripodal aminotriazine-derived polypyridyl ligands with resonative structures as smart starting material may provide a new approach for accessing metal−organic networks or supramolecular complexes with novel fascinating structural patterns and also unexpected properties and/or functions, therefore, giving a new insight into the coordination chemistry. Future work is currently ongoing in this laboratory.

ASSOCIATED CONTENT

Supporting Information

X-ray crystallographic data in CIF format, possible configuration isomers of the *N*-substituted secondary aminotriazine derivatives, NMR spectra, and MALDI-TOF mass spectrum of o-H_3tpat, additional structure diagrams, theory calculation results, TG analyses, and additional magnetic studies. These material are available free of charge via the Internet at http://pubs.acs.org.

AUTHOR INFORMATION

Corresponding Author

*Fax: +886-49-2917956. Tel: +886-49-2910960-4918. E-mail: jyunwu@ncnu.edu.tw (J.-Y.W.), mhchiang@chem.sinica.edu.tw (M.-H.C.), lilai@ncnu.edu.tw (L.-L.L.).

Notes

The authors declare no competing financial interest.

ACKNOWLEDGMENTS

We are grateful to National Chi-Nan University and National Science Council of Taiwan for financial support.

REFERENCES

(1) (a) Lehn, J.-M. *Science* **2002**, *295*, 2400. (b) Reinhoudt, D. N.; Crego-Calama, M. *Science* **2002**, *295*, 2403. (c) Long, J. R.; Yaghi, O. M. *Chem. Soc. Rev.* **2009**, *38*, 1213. (d) Hosseini, M. W. *Acc. Chem. Res.* **2005**, *38*, 313. (e) Perry, J. J., IV; Perman, J. A.; Zaworotko, M. J. *Chem. Soc. Rev.* **2009**, *38*, 1400. (f) Desiraju, G. R. *Acc. Chem. Res.* **2002**, *35*, 565. (g) Kuehl, C. J.; Kryschenko, Y. K.; Radhakrishnan, U.; Seidel, S. R.; Huang, S. D.; Stang, P. J. *Proc. Natl. Acad. Sci. U.S.A.* **2002**, *99*, 4932.

(2) (a) Zerkowski, J. A.; Seto, C. T.; Wierda, D. A.; Whitesides, G. M. *J. Am. Chem. Soc.* **1990**, *112*, 9025. (b) Zerkowski, J. A.; MacDonald, J. C.; Seto, C. T.; Wierda, D. A.; Whitesides, G. M. *J. Am. Chem. Soc.* **1994**, *116*, 2382. (c) Zerkowski, J. A.; Whitesides, G. M. *J. Am. Chem. Soc.* **1994**, *116*, 4298. (d) Mathias, J. P.; Simanek, E. E.; Zerkowski, J. A.; Seto, C. T.; Whitesides, G. M. *J. Am. Chem. Soc.* **1994**, *116*, 4316. (e) Whitesides, G. M.; Simanek, E. E.; Mathlas, J. P.; Seto, C. T.; Chin, D. N.; Mammen, M.; Gordon, D. M. *Acc. Chem. Res.* **1995**, *28*, 37. (f) Ranganathan, A.; Pedireddi, V. R.; Rao, C. N. R. *J. Am. Chem. Soc.* **1999**, *121*, 1752. (g) Staniec, P. A.; Perdigão, L. M. A.; Rogers, B. L.; Champness, N. R.; Beton, P. H. *J. Phys. Chem. C* **2007**, *111*, 886. (h) Ji, H.-F.; Xu, X. *Langmuir* **2010**, *26*, 4620.

(3) (a) Hamblin, J.; Argent, S. P.; Blake, A. J.; Wilson, C.; Champness, N. R. *CrystEngComm* **2008**, *10*, 1782. (b) Gardener, J. A.; Shvarova, O. Y.; Briggs, G. A. D.; Castell, M. R. *J. Phys. Chem. C* **2010**, *114*, 5859.

(4) (a) Thalacker, C.; Miura, A.; de Feyter, S.; de Schryver, F. C.; Würthner, F. *Org. Biomol. Chem.* **2005**, *3*, 414. (b) Silly, F.; Shaw, A. Q.; Castella, M. R.; Briggs, G. A. D. *Chem. Commun.* **2008**, 1907. (c) Yagai, S.; Hamamura, S.; Wang, H.; Stepanenko, V.; Seki, T.; Unoike, K.; Kikkawa, Y.; Karatsu, T.; Kitamura, A.; Würthner, F. *Org. Biomol. Chem.* **2009**, *7*, 3926.

(5) (a) Zhang, X.-L.; Ye, B.-H.; Chen, X.-M. *Cryst. Growth Des.* **2005**, *5*, 1609. (b) Swarbrick, J. C.; Rogers, B. L.; Champness, N. R.; Beton, P. H. *J. Phys. Chem. B* **2006**, *110*, 6110. (c) Walch, H.; Maier, A.-K.; Heckl, W. M.; Lackinger, M. *J. Phys. Chem. C* **2009**, *113*, 1014.

(6) Baisch, U.; Braga, D. *CrystEngComm* **2009**, *11*, 40.

(7) (a) Yagai, S.; Higashi, M.; Karatsu, T.; Kitamura, A. *Chem. Mater.* **2005**, *17*, 4392. (b) Anderson, K. M.; Day, G. M.; Paterson, M. J.; Byrne, P.; Clarke, N.; Steed, J. W. *Angew. Chem., Int. Ed.* **2008**, *47*, 1058.

(8) Shen, J.-S.; Cai, Q.-G.; Jiang, Y.-B.; Zhang, H.-W. *Chem. Commun.* **2010**, *46*, 6786.

(9) (a) Dorta, R.; Stoeckli-Evans, H.; Bodensieck, U.; Süss-Fink, G. *J. Organomet. Chem.* **1998**, *553*, 307. (b) Goodgame, D. M. L.; Hussain, I.; White, A. J. P.; Williams, D. J. *J. Chem. Soc., Dalton Trans.* **1999**, 2899. (c) Sivashankar, K.; Ranganathan, A.; Pedireddi, V. R.; Rao, C. N. R. *J. Mol. Struct.* **2001**, *559*, 41. (d) Nockemann, P.; Meyer, G. *Z. Anorg. Allg. Chem.* **2004**, *630*, 2571. (e) Yu, Y. Q.; Lu, C. Z.; He, X.; Chen, S. M.; Zhang, Q. Z.; Chen, L. J.; Yang, W. B. *J. Chem. Crystallogr.* **2004**, *34*, 905. (f) Chen, C.; Yeh, C. W.; Chen, J. D. *Polyhedron* **2006**, *25*, 1307. (g) Zhang, L.; Zhang, J.; Li, Z.-J.; Cheng, J.-K.; Yin, P.-X.; Yao, Y.-G. *Inorg. Chem.* **2007**, *46*, 5838.

(10) (a) Gamez, P.; de Hoog, P.; Roubeau, O.; Lutz, M.; Driessen, W. L.; Spek, A. L.; Reedijk, J. *Chem. Commun.* **2002**, 1488. (b) Gamez, P.; de Hoog, P.; Lutz, M.; Spek, A. L.; Reedijk, J. *Inorg. Chim. Acta* **2003**, *351*, 319. (c) Gamez, P.; de Hoog, P.; Lutz, M.; Driessen, W. L.; Spek, A. L.; Reedijk, J. *Polyhedron* **2003**, *22*, 205. (d) Gamez, P.; Reedijk, J. *Eur. J. Inorg. Chem.* **2006**, 29.

(11) (a) Demeshko, S.; Dechert, S.; Meyer, F. *J. Am. Chem. Soc.* **2004**, *126*, 4508. (b) Demeshko, S.; Leibeling, G.; Dechert, S.; Meyer, F. *Dalton Trans.* **2004**, 3782.

(12) (a) Barrios, L. A.; Aromí, G.; Frontera, A.; Quiñonero, D.; Deyà, P. M.; Gamez, P.; Roubeau, O.; Shotton, E. J.; Teat, S. J. *Inorg. Chem.* **2008**, *47*, 5873. (b) Yuste, C.; Cañadillas-Delgado, L.; Labrador, A.; Delgado, F. S.; Ruiz-Pérez, C.; Lloret, F.; Julve, M. *Inorg. Chem.* **2009**, *48*, 6630.

(13) (a) de Hoog, P.; Gamez, P.; Roubeau, O.; Lutz, M.; Driessen, W. L.; Spek, A. L.; Reedijk, J. *New J. Chem.* **2003**, *27*, 18. (b) de Hoog, P.; Gamez, P.; Lüken, M.; Roubeau, O.; Krebs, B.; Reedijk, J. *Inorg. Chim. Acta* **2004**, *357*, 213. (c) Casellas, H.; Gamez, P.; Reedijk, J.; Mutikainen, I.; Turpeinen, U.; Masciocchi, N.; Galli, S.; Sironi, A. *Inorg. Chem.* **2005**, *44*, 7918.

(14) Antonioli, B.; Büchner, B.; Clegg, J. K.; Gloe, K.; Gloe, K.; Götzke, L.; Heine, A.; Jäger, A.; Jolliffe, K. A.; Kataeva, O.; Kataev, V.; Klingeler, R.; Krause, T.; Lindoy, L. F.; Popa, A.; Seichter, W.; Wenzel, M. *Dalton Trans.* **2009**, 4795.

(15) Mooibroek, T. J.; Aromí, G.; Quesada, M.; Roubeau, O.; Gamez, P.; George, S. D.; van Slageren, J.; Yasin, S.; Ruiz, E.; Reedijk, J. *Inorg. Chem.* **2009**, *48*, 10643.

(16) (a) Ramírez, J.; Stadler, A.-M.; Kyritsakas, N.; Lehn, J.-M. *Chem. Commun.* **2007**, 237. (b) Melman, G.; Vimal, P.; Melman, A. *Inorg. Chem.* **2009**, *48*, 8662.

(17) Chen, J.; Wang, X.; Shao, Y.; Zhu, J.; Zhu, Y.; Li, Y.; Xu, Q.; Guo, Z. *Inorg. Chem.* **2007**, *46*, 3306.

(18) Mooibroek, T. J.; Aromí, G.; Quesada, M.; Roubeau, O.; Gamez, P.; George, S. D.; van Slageren, J.; Yasin, S.; Mascal, E. M.; Armstrong, A.; Bartberger, M. D. *J. Am. Chem. Soc.* **2002**, *124*, 6274.

(19) Peri, D.; Alexander, J. S.; Tshuva, E. Y.; Melman, A. *Dalton Trans.* **2006**, 4169.

(20) Ghiviriga, I.; Oniciu, D. C. *Chem. Commun.* **2002**, 2718.

(21) Díaz-Ortiz, A.; Elguero, J.; Foces-Foces, C.; de la Hoz, A.; Moreno, A.; Moreno, S.; Sánchez-Migallón, A.; Valiente, G. *Org. Biomol. Chem.* **2003**, *1*, 4451.

(22) (a) Wang, S.-N.; Bai, J.; Xing, H.; Li, Y. Z.; Song, Y.; Pan, Y.; Scheer, M.; You, X.-Z. *Cryst. Growth Des.* **2007**, *7*, 747. (b) Wang, S.-N.; Xing, H.; Bai, J.; Li, Y. Z.; Pan, Y.; Scheer, M.; You, X.-Z. *Chem. Commun.* **2007**, 2293. (c) Wang, S.-N.; Bai, J.; Li, Y.-Z.; Pan, Y.; Scheer, M.; You, X.-Z. *CrystEngComm* **2007**, *9*, 1084.

(23) Gamez, P.; Reedijk, J. *Eur. J. Inorg. Chem.* **2006**, 29.

(24) Tsai, M.-R.; Wu, J.-Y.; Lai, L.-L. *Eur. J. Inorg. Chem.* **2011**, 2172.

(25) Sheldrick, G. M. *SHELX-97* (including *SHELXS* and *SHELXL*); University of Göttingen: Göttingen, Germany, 1997.

(26) *WINGX*: Farrugia, L. J. *J. Appl. Crystallogr.* **1999**, *32*, 837.

(27) (a) Becke, A. D. *J. Chem. Phys.* **1993**, *98*, 1372. (b) Becke, A. D. *J. Chem. Phys.* **1993**, *98*, 5648.

(28) Lee, C.; Yang, W.; Parr, R. G. *Phys. Rev. B* **1988**, *37*, 785.

(29) Frisch, M. J.; Trucks, G. W.; Schlegel, H. B.; Scuseria, G. E.; Robb, M. A.; Cheeseman, J. R.; Montgomery, J. A. Jr.; Vreven, T.; Kudin, K. N.; Burant, J. C.; Millam, J. M.; Iyengar, S. S.; Tomasi, J.; Barone, V.; Mennucci, B.; Cossi, M.; Scalmani, G.; Rega, N.; Petersson, G. A.; Nakatsuji, H.; Hada, M.; Ehara, M.; Toyota, K.; Fukuda, R.; Hasegawa, J.; Ishida, M.; Nakajima, T.; Honda, Y.; Kitao, O.; Nakai, H.; Klene, M.; Li, X.; Knox, J. E.; Hratchian, H. P.; Cross, J. B.; Adamo, C.; Jaramillo, J.; Gomperts, R.; Stratmann, R. E.; Yazyev, O.; Austin, A. J.; Cammi, R.; Pomelli, C.; Ochterski, J. W.; Ayala, P. Y.; Morokuma, K.; Voth, G. A.; Salvador, P.; Dannenberg, J. J.; Zakrzewski, V. G.; Dapprich, S.; Daniels, A. D.; Strain, M. C.; Farkas, O.; Malick, D. K.; Rabuck, A. D.; Raghavachari, K.; Foresman, J. B.; Ortiz, J. V.; Cui, Q.; Baboul, A. G.; Clifford, S.; Cioslowski, J.; Stefanov, B. B.; Liu, G.; Liashenko, A.; Piskorz, P.; Komaromi, I.; Martin, R. L.; Fox, D. J.; Keith, T.; Al-Laham, M. A.; Peng, C. Y.; Nanayakkara, A.; Challacombe, M.; Gill, P. M. W.; Johnson, B.; Chen, W.; Wong, M. W.; Gonzalez, C.; Pople, J. A. *Gaussian 03*, Revision B.04; Gaussian, Inc.: Pittsburgh, PA, 2003.

(30) Harihan, P. C.; Pople, J. A. *Theor. Chim. Acta* **1973**, *28*, 213.
(31) (a) Fan, J.; Sui, B.; Okamura, T.-a.; Sun, W. Y.; Tang, W. X.; Ueyama, N. *J. Chem. Soc., Dalton Trans.* **2002**, 3868. (b) Fan, J.; Zhu, H.-F.; Okamura, T.-a.; Sun, W.-Y.; Tang, W.-X.; Ueyama, N. *Chem.—Eur. J.* **2003**, *9*, 4724. (c) Bar, A. K.; Chakrabarty, R.; Mukherjee, P. S. *Inorg. Chem.* **2009**, *48*, 10880.
(32) Addison, A. W.; Rao, T. N.; Reedijk, J.; van Rijn, J.; Verschoor, G. C. *J. Chem. Soc., Dalton Trans.* **1984**, 1349.
(33) (a) Khanna, S.; Verma, S. *Cryst. Growth Des.* **2012**, *12*, 3025. (b) Park, Y. J.; Sickerman, N. S.; Ziller, J. W.; Borovik, A. S. *Chem. Commun.* **2010**, *46*, 2584. (c) Wu, J.-Y.; Yang, C.-W.; Chen, H.-F.; Jao, Y.-C.; Huang, S.-M.; Tsai, C.; Tseng, T.-W.; Lee, G.-H.; Peng, S.-M.; Lu, K.-L. *J. Solid State Chem.* **2011**, *184*, 1740. (d) Guo, Z.; Cao, R.; Li, X.; Yuan, D.; Bi, W.; Zhu, X.; Li, Y. *Eur. J. Inorg. Chem.* **2007**, 742. (e) Guo, Z.; Li, X.; Gao, S.; Li, Y.; Cao, R. *J. Mol. Struct.* **2007**, *846*, 123. (f) Guo, Z.; Yuan, D.; Bi, W.; Li, X.; Cao, R. *J. Mol. Struct.* **2006**, *782*, 106. (g) Li, Z.; Chen, Y.; Liu, P.; Wang, J.; Huang, M. *J. Solid State Chem.* **2005**, *178*, 2306. (h) Deng, Q.-J.; Zeng, M.-H.; Liang, H.; Ng, S. W.; Huang, K.-L. *Acta Crystallogr., Sect. E* **2006**, *62*, m1293. (i) Deng, Q.-J.; Zeng, M.-H.; Liang, H.; Huang, K.-L. *Chin. J. Struct. Chem.* **2006**, *25*, 975.
(34) (a) Chiari, B.; Piovesana, O.; Tarantelli, T.; Zanazzi, P. F. *Inorg. Chem.* **1993**, *32*, 4834. (b) Papadopoulos, A. N.; Tangoulis, V.; Raptopoulou, C. P.; Terzis, A.; Kessissoglou, D. P. *Inorg. Chem.* **1996**, *35*, 559. (c) Ayllón, J. A.; Santos, I. C.; Henriques, R. T.; Almeida, M.; Alcácer, L.; Duarte, M. T. *Inorg. Chem.* **1996**, *35*, 168. (d) Menon, S.; Rajasekharan, M. V.; Tuchagues, J. P. *Inorg. Chem.* **1997**, *36*, 4341.
(35) O'Connor, C. J. *Prog. Inorg. Chem.* **1982**, *29*, 203.
(36) (a) Marsh, W. E.; Patel, K. C.; Hatfield, W. E.; Hodgson, D. J. *Inorg. Chem.* **1983**, *22*, 511. (b) Hatfield, W. E.; MacDougall, J. J.; Shepherd, R. E. *Inorg. Chem.* **1981**, *20*, 4216. (c) Hatfield, W. E.; Weller, R. R.; Hall, J. W. *Inorg. Chem.* **1980**, *19*, 3825. (d) Hatfield, W. E. *Comments Inorg. Chem.* **1981**, *1*, 105. (e) Marsh, W. E.; Hatfield, W. E.; Hodgson, D. J. *Inorg. Chem.* **1982**, *21*, 2679. (f) Balagopalakrishna, C.; Rajasekharan, M. V. *Phys. Rev. B: Condens. Matter* **1990**, *42*, 7794.
(37) (a) Toulouse, G. *Commun. Phys.* **1977**, *2*, 115. (b) Liu, J.; Koo, C.; Amjad, A.; Feng, P. L.; Choi, E.-S.; del Barco, E.; Hendrickson, D. N.; Hill, S. *Phys. Rev. B: Condens. Matter* **2011**, *84*, 094443/1−094443/10. (c) Mukherjee, S.; Bagai, R.; Abboud, K. A.; Christou, G. *Inorg. Chem.* **2011**, *50*, 3849. (d) Wang, Y.-Q.; Zhang, X.-M.; Li, X.-B.; Wang, B.-W.; Gao, E.-Q. *Inorg. Chem.* **2011**, *50*, 6314. (e) Yang, E.-C.; Liu, Z.-Y.; Li, Y.-L.; Wang, J.-Y.; Zhao, X.-J. *Dalton Trans.* **2011**, *40*, 8513. (f) Anwar, M. U.; Thompson, L. K.; Dawe, L. N. *Dalton Trans.* **2011**, *40*, 1437.
(38) Meyer, A.; Gleizes, A.; Girerd, J. J.; Verdaguer, M.; Kahn, O. *Inorg. Chem.* **1982**, *21*, 1729.